IFAC Symposium on Power Plants and Power Systems Control, Kananaskis, Canada, 2006

COMPLETE FAULT ANALYSIS FOR LONG TRANSMISSION LINE USING SYNCHRONIZED SAMPLING

Nan Zhang * **Mladen Kezunovic** *

* *Texas A&M University, Department of Electrical and Computer Engineering, College Station, TX 77843-3128, U.S.A.*

Abstract: A complete fault analysis scheme for long transmission line represented with distributed parameters is proposed in this paper. The synchronized samples from both ends of the transmission line are the data sources for this scheme. The paper derives a specific feature which equals to zero for normal situation and external faults, and is close to fault current during the internal faults. This feature is used for fault detection and classification. Fault location is then implemented by selecting different methods according to the classified fault type. The results from a comprehensive evaluation study demonstrate an excellent performance of entire fault analysis. *Copyright ©2006 IFAC*

Keywords: fault analysis, fault detection, fault classification, fault location, synchronized sampling.

1. INTRODUCTION

Automated fault analysis tool for transmission lines is very useful for on-line confirmation and off-line trouble-shooting. When it is used on-line, the system operator can obtain the detailed information about the disturbances before he issues corrective controls. It can help correct the relay misoperations as soon as possible to prevent the occurrence of a large-scale blackout. When used off-line, the disturbances can be fully analyzed and the relay system operations can be assessed in a very detailed way.

With the fast development of signal processing, computer and communication technologies, new approaches have been deployed in the fault analysis providing better solutions in fault detection, classification and location. An expert system based approach is described in (Girgis and Johns, 1996) and a phasor measurement unit (PMU) based approach is described in (Jiang *et al.*, 2003). Those approaches depend on the phasor calculation. A neural network based fault analysis tool is developed in (Oleskovicz *et al.*, 2001), but it is hard to precisely obtain a fault location since neural network is not good at precisely classifying the continuous variables. Methods based on traveling waves and recently based on fault-generated high-frequency transients have been used extensively in protection schemes (Chamia and Liberman, 1978; Bo *et al.*, 2000). Most of those techniques require very high-speed sampling rate which is still not widely used in existing devices.

A time-domain fault location technique was developed at Texas A&M University (Kezunovic *et al.*, 1994). The digital fault recorder with Global Positioning System (GPS) satellite receiver is the source of the data for this approach. Data from both ends of transmission line are used to achieve high accuracy of the fault location. This method will be more attractive when the concept of Wide

Area Measurement System (WAMS) and Phasor Measurement Unit (PMU) are further developed.

Previous efforts were aimed at implementing accurate fault location algorithms for short line represented with lumped parameters and long line represented with distributed parameters (Kezunovic *et al.*, 1994; Gopalakrishnan and Kezunovic, 2000). A complete fault analysis tool was proposed for short line (Kezunovic and Perunicic, 1996). Due to the effect of shunt capacitances in long line, the wave propagation and the fault analysis principle is quite different from those in the short line algorithm. The development of fault analysis scheme can not shift to the long line model directly. In this paper, a complete fault analysis scheme including fault detection, classification and location is developed specially for long transmission line model. The paper first derives the theoretical basis in detail, and then designs the complete fault analysis scheme according to the derivation in the theoretical basis. At the end, a comprehensive evaluation study is implemented to evaluate the statistical performance of the proposed approach.

2. THEORETICAL BASIS

2.1 Feature Extraction using Synchronized Sampling

For long transmission line represented by distributed parameters, the voltage and current along the line are functions of the distance x and the time t,

$$\begin{aligned}\frac{\partial v(x,t)}{\partial x} &= -Ri(x,t) - L\frac{\partial i(x,t)}{\partial t}\\ \frac{\partial i(x,t)}{\partial x} &= -C\frac{\partial v(x,t)}{\partial t}\end{aligned} \tag{1}$$

where R, L, C are per-unit-length resistance, inductance and capacitance respectively. A discrete form of the solution of (1) is derived as follows (Gopalakrishnan and Kezunovic, 2000):

$$\begin{aligned}v_j(k) = {} & \frac{1}{2}\left[v_{j-1}(k-1) + v_{j-1}(k+1)\right]\\ & + \frac{Z_c}{2}\left[i_{j-1}(k-1) - i_{j-1}(k+1)\right]\\ & - \frac{R\triangle x}{4}\left[i_{j-1}(k-1) + i_{j-1}(k+1)\right] - \frac{R\triangle x}{2}i_j(k)\end{aligned} \tag{2}$$

$$\begin{aligned}i_j(k) = {} & \frac{1}{2Z_c}\left[v_{j-1}(k-1) - v_{j-1}(k+1)\right]\\ & + \frac{1}{2}\left[i_{j-1}(k-1) + i_{j-1}(k+1)\right]\\ & + \frac{R\triangle x}{4Z_c}\left[i_{j-1}(k+1) - i_{j-1}(k-1)\right]\end{aligned} \tag{3}$$

where $\triangle x = \triangle t/\sqrt{LC}$ is the distance that the wave travels with a sampling time step $\triangle t$; $Z_c = \sqrt{L/C}$ is the surge impedance. Subscript j is the position of the discretized point of the line and k is the sample point.

The two equations define the relation of voltage and current samples between two points on the transmission line with the distance of $\triangle x$, as shown in Fig. 1. Combining (2) and (3) to eliminate $v_{j-1}(k+1)$ and $i_{j-1}(k+1)$, we get

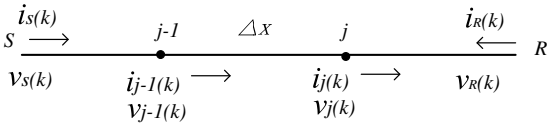

Fig. 1. A homogeneous transmission line

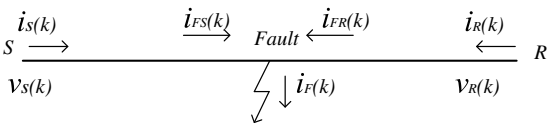

Fig. 2. A faulted transmission line

$$i_j(k)\left[1 + \frac{R\triangle x}{2Z_c}\right] + \frac{v_j(k)}{Z_c} = \frac{v_{j-1}(k-1)}{Z_c} + i_{j-1}(k-1)\left[1 - \frac{R\triangle x}{2Z_c}\right] \tag{4}$$

When there is no internal fault on the line, which means the line parameters are homogeneous, equation (4) can be expressed as the relation between the sending end and receiving end samples. Substitute $j-1$ with S and j with R and note the direction of I_R . Equation (4) is changed to

$$-i_R(k)\left[1 + \frac{Rd}{2Z_c}\right] + \frac{v_R(k)}{Z_c} = \frac{v_S(k-P)}{Z_c} + i_S(k-P)\left[1 - \frac{Rd}{2Z_c}\right] \tag{5}$$

where d is the length of the transmission line, P is the sample difference if the wave travels from the sending end to the receiving end with the time of $P\triangle t$. Define

$$\begin{aligned}i_{d1}(k) = {} & i_S(k-P)\left[1 - \frac{Rd}{2Z_c}\right] + i_R(k)\left[1 + \frac{Rd}{2Z_c}\right]\\ & + \frac{v_S(k-P)}{Z_c} - \frac{v_R(k)}{Z_c}\end{aligned} \tag{6}$$

Similarly, we can get another form of equation (5) as

$$-i_S(k)\left[1 + \frac{Rd}{2Z_c}\right] + \frac{v_S(k)}{Z_c} = \frac{v_R(k-P)}{Z_c} + i_R(k-P)\left[1 - \frac{Rd}{2Z_c}\right] \tag{7}$$

And define

$$\begin{aligned}i_{d2}(k) = {} & i_R(k-P)\left[1 - \frac{Rd}{2Z_c}\right] + i_S(k)\left[1 + \frac{Rd}{2Z_c}\right]\\ & + \frac{v_R(k-P)}{Z_c} - \frac{v_S(k)}{Z_c}\end{aligned} \tag{8}$$

When there is no internal fault on the line, obviously $i_{d1}(k)$ and $i_{d2}(k)$ should equal to zero.

Now consider the situation of an internal fault. As shown in Fig. 2, at a certain time, the fault current and voltage at the fault point can be expressed as the signals from sending end and receiving end:

$$\begin{aligned}i_F(k) &= i_{FS}(k) + i_{FR}(k)\\ v_F(k) &= v_{FS}(k) = v_{FR}(k)\end{aligned} \tag{9}$$

Note that for long transmission line, $i_S(k) \neq i_{FS}(k)$ and $i_R(k) \neq i_{FR}(k)$ due to the traveling wave issue. According to equation (5), if we note

the current direction for each current signal shown in Fig. 2, we have

$$\frac{v_S(k-P_S)}{Z_c} + i_S(k-P_S)\left[1-\frac{Rd_S}{2Z_c}\right] = i_{FS}(k)\left[1+\frac{Rd_S}{2Z_c}\right] + \frac{v_{FS}(k)}{Z_c} \tag{10}$$

$$-i_R(k)\left[1+\frac{Rd_R}{2Z_c}\right] + \frac{v_R(k)}{Z_c} = \frac{v_{FR}(k-P_R)}{Z_c} - i_{FR}(k-P_R)\left[1-\frac{Rd_R}{2Z_c}\right] \tag{11}$$

where P_S and P_R are the sample differences if the wave travels from the fault point to the sending end with the time of $P_S\triangle t$ and to the receiving end with the time of $P_R\triangle t$ respectively. d_S and d_R are the distances from the fault point to the sending end and to the receiving end respectively.

Substitute k with $k-P_R$ in equation (10), and minus equation (11) to eliminate $v_F(k-P_R)$. Note that $P=P_S+P_R$ and $d=d_S+d_R$, then the left-hand side is changed to

$$\begin{aligned} &i_S(k-P)\left[1-\frac{Rd}{2Z_c}\right] + i_R(k)\left[1+\frac{Rd}{2Z_c}\right] + \frac{v_S(k-P)}{Z_c} \\ &-\frac{v_R(k)}{Z_c} + i_S(k-P)\frac{Rd_R}{2Z_c} - i_R(k)\frac{Rd_S}{2Z_c} \\ &= i_{d1}(k) + i_S(k-P)\frac{Rd_R}{2Z_c} - i_R(k)\frac{Rd_S}{2Z_c} \end{aligned} \tag{12}$$

And the right-hand side is changed to

$$\begin{aligned} &i_{FS}(k-P_R)\left[1+\frac{Rd_S}{2Z_c}\right] + i_{FR}(k-P_R)\left[1-\frac{Rd_R}{2Z_c}\right] \\ &= i_F(k-P_R) + i_{FS}(k-P_R)\frac{Rd_S}{2Z_c} - i_{FR}(k-P_R)\frac{Rd_R}{2Z_c} \end{aligned} \tag{13}$$

For realistic transmission line, $\frac{Rd_S}{2Z_c} \ll 1$ and $\frac{Rd_R}{2Z_c} \ll 1$, then

$$i_{d1}(k) \approx i_F(k-P_R) \tag{14}$$

Similarly, if we start from equation (7), we can get

$$i_{d2}(k) \approx i_F(k-P_S) \tag{15}$$

With the help of synchronized sampling, the current and voltage samples used for calculating $i_{d1}(k)$ or $i_{d2}(k)$ are available from the both ends of transmission line. In our fault analysis scheme, $i_{d1}(k)$ is used as the main feature for long line model in fault detection and classification. The equations (2) and (3) are the recursive equations used for fault location.

2.2 Three-phase Calculation

For a three-phase system, all the line parameters and the measured voltage and current signals should be transformed into modal domain first to get the decoupled systems and the derivation in previous section is still fulfilled for each modal component.

First of all, use transformation matrix T to transfer the line parameters and the measured phase values into the modal domain,

$$T = \frac{1}{\sqrt{3}}\begin{bmatrix} 1 & \sqrt{2} & 0 \\ 1 & -1/\sqrt{2} & \sqrt{3}/\sqrt{2} \\ 1 & -1/\sqrt{2} & -\sqrt{3}/\sqrt{2} \end{bmatrix} \tag{16}$$

$$inv(T) = \frac{1}{\sqrt{3}}\begin{bmatrix} 1 & 1 & 1 \\ \sqrt{2} & -1/\sqrt{2} & -1/\sqrt{2} \\ 0 & \sqrt{3}/\sqrt{2} & -\sqrt{3}/\sqrt{2} \end{bmatrix} \tag{17}$$

$$[Z,Y]_{0,1,2} = inv(T)[Z,Y]_{a,b,c}T \tag{18}$$

$$[v(k),i(k)]_{a-0,1,2} = inv(T)\begin{bmatrix} [v(k),i(k)]_a \\ [v(k),i(k)]_b \\ [v(k),i(k)]_c \end{bmatrix} \tag{19}$$

It is noted that the transformation matrix T and its inverse matrix have the unsymmetrical form. From equation (19), we can get the modal components with respect to the reference phase "a". Similarly, we can get the modal components with respect to the phases "b" and "c" by rotation. Note that the 0-mode has the same form irrespective what the reference phase is. We can get seven sets of modal components:

$$[v(k),i(k)]_0; [v(k),i(k)]_{a-1,2}; [v(k),i(k)]_{b-1,2}; [v(k),i(k)]_{c-1,2} \tag{20}$$

Those components will be selected for the uses in fault detection, classification and location. From the sequence network analysis, we can find the availability of each modal component to detect the different fault type, as shown in Table 1. It is noted that there is no unique modal component that can be used to detect all the fault types. That should be noted when designing the fault analysis algorithms.

3. FAULT ANALYSIS SCHEME

3.1 Fault Detection

Define

$$I_{d1-m} = \frac{\sum_j |i_{d1}(j)|_m}{N}; \qquad j = k-N+1, k-N+2, \ldots, k \tag{21}$$

Table 1. Availability of different modal components to correctly detect the different fault type

	0	$a1$	$a2$	$b1$	$b2$	$c1$	$c2$
AG	√	√	×	√	√	√	√
BG	√	√	√	√	×	√	√
CG	√	√	√	√	√	√	×
AB	×	√	√	√	√	×	√
BC	×	×	√	√	√	√	√
CA	×	√	√	×	√	√	√
ABG	√	√	√	√	√	√	√
BCG	√	√	√	√	√	√	√
CAG	√	√	√	√	√	√	√
ABC	×	√	√	√	√	√	√

where m is the related modal component, N is the number of samples in one cycle. The criterion for detecting an internal fault is given as

$$max[I_{d1-a-1}, I_{d1-b-1}, I_{d1-c-1}] \geq T_1 \qquad (22)$$

In equation (22), a threshold is set to tolerate the model and measurement imperfection. The average value of $i_{d1}(k)$ in one cycle is compared to that threshold. The calculation is carried out using "a-1", "b-1" and "c-1" modal components.

3.2 Fault Classification

Through sequence network analysis with different boundary conditions, we can find the features for classifying the fault types using different modal components (Ge, 1993), as shown in Table 2. The entries in the table are the modal fault current components at the fault point. As derived in equation (14), $i_{d1}(k)$ is directly related to the fault current with several samples delay. Therefore, we can use $i_{d1}(k)$ to design the fault classification scheme according to the Table 2.

The flowchart of fault classification is shown in Fig. 3, where i_{d1-m} has identical definition as equation (21). The thresholds T_2 and T_3 are set to tolerate the model and measurement imperfection, as well as the algorithm approximation.

3.3 Fault Location

The fault location calculation follows the methods shown in Fig 4. According to the fault type, the calculation will based on the selection of the prominent modal components to achieve an accurate result. The selection scheme is as follows:

- For ground fault (AG, BG, CG, ABG, BCG, CAG), the calculation is implemented using "mode 0" components. The obtained fault location is the final one.
- For AB fault, the calculation is implemented using "a-1" and "b-1" modal components. The final fault location is the average of the two results.
- For BC fault, the calculation is implemented using "b-1" and "c-1" modal components. The final fault location is the average of the two results.
- For CA fault, the calculation is implemented using "c-1" and "a-1" modal components. The final fault location is the average of the two results.
- For three-phase fault, the calculation is implemented using "a-1", "b-1" and "c-1" modal components. The final fault location is the average of the three results.

Table 2. Features for classification of different fault type

Fault Type	Features
AG	$I_{F-0} \neq 0; \quad I_{F-a-2} = 0$
BG	$I_{F-0} \neq 0; \quad I_{F-b-2} = 0$
CG	$I_{F-0} \neq 0; \quad I_{F-c-2} = 0$
AB	$I_{F-0} = 0; \quad I_{F-c-1} = 0$
BC	$I_{F-0} = 0; \quad I_{F-a-1} = 0$
CA	$I_{F-0} = 0; \quad I_{F-b-1} = 0$
ABG	$I_{F-0} \neq 0; \quad I_{F_0} + I_{F-c-1} = 0$
BCG	$I_{F-0} \neq 0; \quad I_{F_0} + I_{F-a-1} = 0$
CAG	$I_{F-0} \neq 0; \quad I_{F_0} + I_{F-b-1} = 0$
ABC	$I_{F-0} = 0; I_{F-a-1} \neq 0;$ $I_{F-b-1} \neq 0; I_{F-c-1} \neq 0$

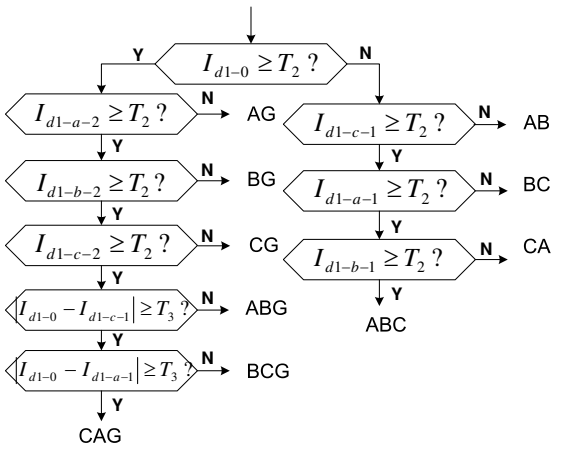

Fig. 3. Flowchart of fault classification

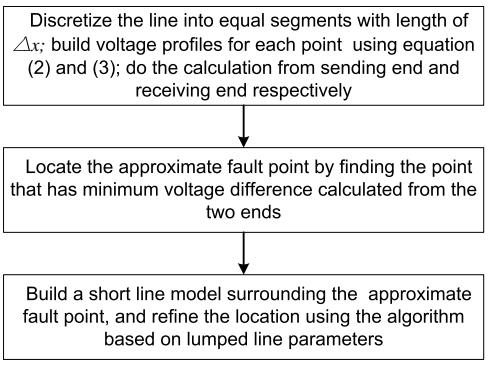

Fig. 4. Procedure of fault location

3.4 Implementation of Entire Fault Analysis Scheme

The entire fault analysis including fault detection, classification and location can be implemented in the same software package. The flowchart is shown in Fig. 5. The data window used for calculation is one cycle, and the data window is moving forward with selected time step $\triangle t$. The fault is detected if the equation (22) is fulfilled for a successive cycle. Then the post-fault values are used for fault classification and fault location, using the methods demonstrated in the previous sections.

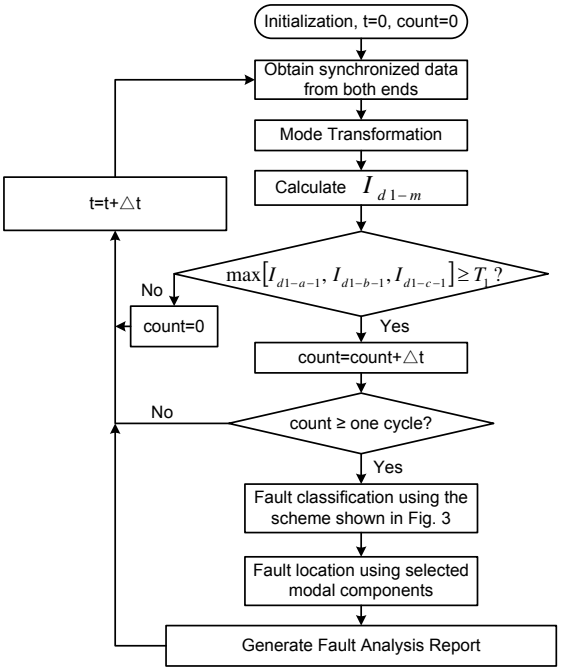

Fig. 5. Flowchart of fault diagnosis scheme using synchronized sampling

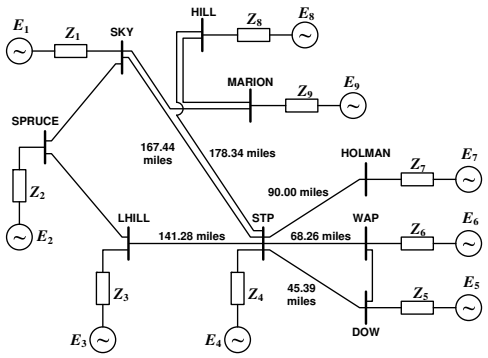

Fig. 6. CenterPoint Energy STP-SKY model

4. MODEL IMPLEMENTATION AND PERFORMANCE EVALUATION

4.1 Power System Models

The proposed fault analysis scheme is evaluated using Alternative Transient Program (ATP) (*Alternative Transients Program (ATP) - Rule Book*, 1992). An actual 345kV power system section from CenterPoint Energy (Ristanovic *et al.*, 2001) is used for various fault event simulations. The STP-SKY line is the line of interest in this study, which is shown in Fig. 6.

4.2 Generation of Test Scenarios

The performance evaluation is based on randomly generated fault scenarios, which can demonstrate the statistical performance and robustness of the proposed scheme in all kinds of situations. There are five test sets generated in our study with 500 scenarios each, as shown in Table 3. For each test set, the fault parameters are randomly selected from uniform distribution of: all fault types, fault distances $(0-100\%)$, fault resistances $(0-50\Omega)$, and fault inception angles $(0-180^0)$.

Table 3. Test sets for performance study

Set	Description	Condition	Cases
1	Norm	Normal Condition	500
2	Weak-infeed	Disconnect E1 and E9	500
3	Phase-shift	E1 with phase shift -30^0	500
4	Freq-shift	System Frequency of $59Hz$	500
5	External	External Faults	500

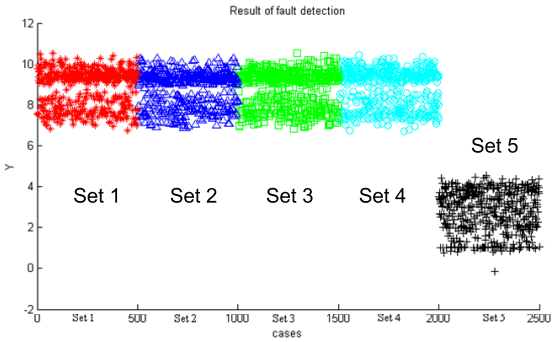

Fig. 7. Result of fault detection

4.3 Test Results and Discussions

The test result shown in this section is based on the sampling rate of $20KHz$. The sampling rate does not affect the performance of fault detection and fault classification, but it will affect the accuracy of fault location. From Fig. 4, we know that if the sampling rate is higher, we can discretize the line into more segments. When building the short line model, the suspect area is narrowed to a small section of the transmission line. The error of fault location is not expected to be large then.

The correctness rate of fault detection and classification are 100% for all given test sets. The result of fault detection is shown in Fig. 7. The horizontal axis is the scenarios in the five test sets, and the vertical axis is defined as:

$$Y = ln\{max[I_{d1-a-1}, I_{d1-b-1}, I_{d1-c-1}]\} \qquad (23)$$

It is seen that the values of Y for the internal faults scenarios (Set1-Set4) are well differentiable from the values for the external faults cases (Set5). Hence the threshold T_1 in equation (22) is very easy to set. Similarly, the thresholds T_2 and T_3 in fault classification are also easy to select.

An example of fault classification is shown in Table 4. The entries are calculated I_{d1-m} with different modal components in ten fault types. We can compare with Fig. 3 to see the efficiency of the proposed approach.

Table 4. An example of fault classification result

	0	$a1$	$b1$	$c1$	$a2$	$b2$	$c2$
AG	4.50E+03	9.06E+03	4.53E+03	4.53E+03	3.93	4.53E+03	4.53E+03
BG	5.91E+03	5.82E+03	1.16E+04	5.81E+03	5.81E+03	3.95	5.81E+03
CG	5.04E+03	5.15E+03	5.15E+03	1.03E+04	5.15E+03	5.15E+03	3.81
AB	1.04E-03	2.56E+04	2.56E+04	7.02	8.54E+03	8.54E+03	1.71E+04
BC	1.06E-03	6.66	2.74E+04	2.74E+04	1.82E+04	9.13E+03	9.13E+03
CA	1.16E-03	2.10E+04	6.66	2.10E+04	7.01E+03	1.40E+04	7.02E+03
ABG	3.52E+03	2.54E+04	2.60E+04	3.47E+03	9.06E+03	8.43E+03	1.71E+04
BCG	3.06E+03	3.08E+03	2.80E+04	2.69E+04	1.83E+04	8.72E+03	9.81E+03
CAG	4.03E+03	2.06E+04	3.98E+03	2.16E+04	7.73E+03	1.40E+04	6.81E+03
ABC	3.21E-04	2.53E+04	3.31E+04	2.75E+04	1.83E+04	1.40E+04	1.71E+04

For almost 90% of the scenarios, the fault location error is under 2%. The error of fault location for a single fault scenario is defined as:

$$\text{error}(\%) = \frac{|\text{Actual Location - Computed Location}|}{\text{Line Length}} \quad (24)$$

The average error for internal fault cases Set1-Set4 are 0.547%, 0.576%, 0.528% and 0.539% respectively, corresponding to about 0.8 mile with respect to the line length of 167.44 miles. The performance of fault location is less affected by different fault parameters, system operating conditions. The results show the consistency of the algorithm for each test set. That is one of the advantages using two-end synchronized data.

5. CONCLUSION

This paper proposes a complete fault analysis tool for long transmission line with distributed parameters. The calculation is carried out in the time domain, therefore the calculation of a phasor is not an issue in the proposed approach. With the availability of the synchronized data from two ends, the fault analysis can be very accurate. The proposed scheme can be implemented in an integrated software package as an add-on function for digital fault recorder. The comprehensive study in this paper proves the excellent performance of the proposed fault analysis tool.

REFERENCES

Alternative Transients Program (ATP) - Rule Book (1992). CanAm EMTP User Group, Portland, OR.

Bo, Z. Q., F. Jiang, Z. Chen, X. Dong, G. Weller and M. A. Redfern (2000). Transient based protection for power transmission systems. In: *Proc. IEEE PES Winter Meeting*. Vol. 3. Singapore. pp. 1832–1837.

Chamia, M. and S. Liberman (1978). Ultra high speed relay for EHV/UHV transmission lines – development, design and application. *IEEE Trans. Power Apparatus and Systems* **97**, 2104–2112.

Ge, Y. (1993). *New Types of Protective Relaying and Fault Location Theory and Techniques*. Xi'an Jiaotong University Press. Xi'an, China.

Girgis, A. A. and M. B. Johns (1996). A hybrid expert system for faulted section identification, fault type classification and selection of fault location algorithms. *IEEE Trans. Power Delivery* **4**(2), 978–985.

Gopalakrishnan, A. and M. Kezunovic (2000). Fault location using distributed parameter transmission line model. *IEEE Trans. Power Delivery* **15**(4), 1169–1174.

Jiang, J., C. Chen and C. Liu (2003). A new protection scheme for fault detection, directiondiscrimination, classification, and location in transmission lines. *IEEE Trans. Power Delivery* **18**(1), 34–42.

Kezunovic, M. and B. Perunicic (1996). Automated transmission line fault analysis using synchronized sampling at two ends. *IEEE Trans. Power Systems* **11**(1), 441–447.

Kezunovic, M., B. Perunicic and J. Mrkic (1994). An accurate fault location algorithm using synchronized sampling. *Electric Power Systems Research Journal* **29**(3), 161–169.

Oleskovicz, M., D. V. Coury and R. K. Aggarwal (2001). A complete scheme for fault detection, classification and location in transmission lines using neural networks. In: *Proc. IEE Seventh Int. Conf. on Developments in Power System Protection*. pp. 335–338.

Ristanovic, D., S. Vasilic and M. Kezunovic (2001). Design and implementation of scenarios for evaluating and testing distance relays. In: *Proc. North American Power Symp.*. College Station, TX. pp. 185–192.